Analytica Chimica Acta 636 (2009) 19–27

Contents lists available at ScienceDirect

Analytica Chimica Acta

journal homepage: www.elsevier.com/locate/aca

Simultaneous determination of adenine guanine and thymine at multi-walled carbon nanotubes incorporated with poly(new fuchsin) composite film

Ching Tang, Umasankar Yogeswaran, Shen-Ming Chen*

Department of Chemical Engineering and Biotechnology, National Taipei University of Technology, No.1, Section 3, Chung-Hsiao East Road, Taipei 106, Taiwan, ROC

ARTICLE INFO

Article history:
Received 9 December 2008
Received in revised form 22 January 2009
Accepted 26 January 2009
Available online 4 February 2009

Keywords:
Multiwall carbon nanotubes
Composite film
Modified electrodes
Electrocatalysis
Deoxyribonucleic acid (DNA)
Adenine
Guanine
Thymine

ABSTRACT

A composite film (MWCNTs–PNF) which contains multi-walled carbon nanotubes (MWCNTs) along with the incorporation of poly(new fuchsin) (PNF) has been synthesized on glassy carbon electrode (GCE), gold (Au) and indium tin oxide (ITO) by potentiostatic methods. The presence of MWCNTs in the composite film enhances surface coverage concentration (Γ) of PNF to ≈176.5%, and increases the electron transfer rate constant (k_s) to ≈346%. The composite film also exhibits promising enhanced electrocatalytic activity towards the mixture of biochemical compounds such as adenine (AD), guanine (GU) and thymine (THY). The surface morphology of the composite film deposited on ITO has been studied using scanning electron microscopy and atomic force microscopy. These two techniques reveal that the PNF incorporated on MWCNTs. Electrochemical quartz crystal microbalance study reveals the enhancement in the functional properties of MWCNTs and PNF. The electrocatalytic responses of analytes at MWCNTs and MWCNTs–PNF films were measured using both cyclic voltammetry (CV) and differential pulse voltammetry (DPV). From electrocatalysis studies, well separated voltammetric peaks have been obtained at the composite film for AD, GU and THY, with the peak separation of 320.3 and 132.7 mV between GU–AD and AD–THY respectively. The sensitivity of the composite film towards AD, GU and THY in DPV technique is 218.18, 12.62 and 78.22 mA M^{-1} cm^{-2} respectively, which are higher than MWCNTs film. Further, electroanalytical studies of AD, GU and THY present in single-strand deoxyribonucleic acid (ssDNA) have been carried out using semi-derivative CV and DPV.

1. Introduction

Electropolymerization is a simple but powerful method in targeting selective modification of different types of electrodes with desired matrices. However, the materials on the matrices do not possess peculiar properties when compared with those materials which are chemically synthesized by traditional methods. The electroactive polymers and carbon nanotube (CNT) matrices have received considerable attraction in recent years. Numerous conjugated polymers were electrochemically synthesized for their application in the chemical and biochemical sensor devices [1]. These conjugated polymers exhibit an interesting enhancement in the electrocatalytic activity towards the oxidation or reduction of several biochemical and inorganic compounds [2] where, some functional groups in the polymers act as catalyst [3-5]. The word "enhanced electrocatalytic activity" could be explained as: both increase in peak current and lower in over potential [6]. A group of conjugated polymers representing azines such as phenazines, phenothiazines, phenoxazines, etc., are the examples of redox indicators and mediators used in bioelectrochemistry [7]. The electropolymerization of azine group compounds are usually performed by anodic oxidation in acidic medium [8-10]. Similarly, the triphenylmethane derivative, new fuchsin (NF), also known as basic fuchsin and magenta III, is a dye and an acid–base indicator. NF has been used to determine sulfide ions by kinetic spectrophotometric method [11], as a copper corrosion inhibitor [12], and as a photosensitive reagent [13]. The molecular structure of NF is given in Scheme 1. Literature reveals that attempts have been made for the electropolymerization of NF and application of poly(new fuchsin) (PNF) for the electrocatalysis of halogen and sulfur oxyanions [14–16]. The same studies reported also, PNF forms thin films with high stability. Further, the PNF deposition on electrodes is useful as an electron transfer mediator [14,15]. In some reports, NF is also considered as low or non-toxic [17]. For example, Yang et al. studied the interaction between fuchsin and DNA [18].

Varieties of applications of CNT matrices for the detection of inorganic and bioorganic compounds were already reported [19–21]. Even though, electrocatalytic activity of the conjugated polymers and CNTs matrices individually shows good result; some properties like mechanical stability, sensitivity for different techniques and electrocatalysis of multiple compounds are found to be poor. To overcome this difficulty, new studies have been devel-

* Corresponding author. Tel.: +886 2270 17147; fax: +886 2270 25238.
E-mail address: smchen78@ms15.hinet.net (S.-M. Chen).

0003-2670/$ – see front matter © 2009 Elsevier B.V. All rights reserved.
doi:10.1016/j.aca.2009.01.055

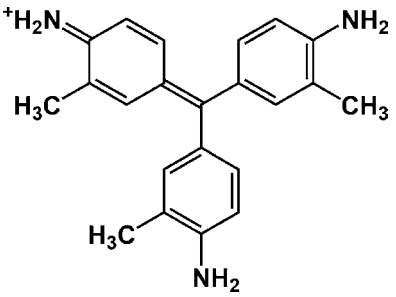

Scheme 1. Molecular structure of NF.

oped in the past decade by preparing composite films composed of both CNTs and conjugated polymers. The rolled-up graphene sheets of carbon exhibit a π-conjugative structure with a highly hydrophobic surface. This unique property of CNTs allows them to interact with some organic aromatic compounds through π–π electronic and hydrophobic interactions and form new structures [22,23]. There were past attempts in the preparation of composite and sandwiched films for electrocatalytic studies such as selective detection of dopamine in the presence of ascorbic acid [24]. The sandwiched films were also been used for the designing of nanodevices with the help of non-covalent adsorption, electrodeposition, etc. [25]. Similar previous studies on CNT–polymer composites show the necessity of polymer on the CNTs, such as improvement in functional properties like orientation, enhanced electron transport (higher conductivity), high capacitance, etc. [26,27].

Adenine (AD), guanine (GU) and thymine (THY) are the important components found in deoxyribonucleic acid (DNA). Determination of individual concentrations of AD, GU and THY or their ratio in DNA is important for the measurement of nucleic acid concentration itself [28]. Thus, the determination of these analytes is pharmacologically necessary using chemically modified electrodes, which are done by means of electrocatalysis [29,30]. The previously attempted methods for determination of these analytes have problems like irreversible adsorption of purine bases on the electrode surface and have led to surface fouling [31]. Recently, two methods based on electrochemical GU and colloidal gold nanoparticles have been reviewed and compared with the existing genotyping methods [32]. Not only limited to these, the electrochemical genosensing properties of gold nanoparticles with CNT hybrid film and polycrystalline gold electrodes were also reported [33,34]. Further, the label-free electrochemical detection of DNA hybridization on gold electrode and the oxidation signal of GU have also been monitored [29,35-36].

The literature survey reveals that there were no attempts reported for the synthesis of composite film composed of CNTs and PNF for sensor applications. In this paper, we report about a novel composite film (MWCNTs–PNF) made of multi-walled carbon nanotubes (MWCNTs) which have incorporated PNF. Composite's characterization, enhancement in functional properties, peak current and electrocatalytic activity have also been reported along with its application in the simultaneous determination of AD, GU and THY present in single strand deoxyribonucleic acid (ssDNA). The film formation process involves the modification of glassy carbon electrode (GCE) with uniformly well dispersed MWCNTs, and which is then modified with PNF.

2. Experimental

2.1. Materials

NF, MWCNTs (OD = 10–20 nm, ID = 2–10 nm and length = 0.5–200 μm), AD, GU, THY and ssDNA bought from Aldrich and Sigma–Aldrich were used as received. All other chemicals used were of analytical grade. The preparation of aqueous solution was done with twice distilled deionized water. Solutions were deoxygenated by purging with pre-purified nitrogen gas. Buffer solutions were prepared from potassium hydrogen phthalate (KHP) for pH 4, KOH for pH 13 and phosphate buffer (PBS) (0.1 M Na_2HPO_4 and 0.1 M NaH_2PO_4) for pH 7.4 aqueous solutions.

2.2. Apparatus

Cyclic voltammetry (CV), semi-derivative cyclic voltammetry (SDCV) and differential pulse voltammetry (DPV) were performed in analytical system models CHI-1205, CHI-410a and CHI-750 potentiostats respectively. A conventional three-electrode cell assembly consisting of an Ag/AgCl reference electrode and a Pt wire counter electrode were used for the electrochemical measurements. The working electrode was either an unmodified GCE or a GCE modified with PNF, MWCNTs or MWCNTs–PNF films; all the potentials were reported versus Ag/AgCl reference electrode. The working electrode for electrochemical quartz crystal microbalance (EQCM) measurements was an 8 MHz AT-cut quartz crystal coated with gold electrode. The diameter of the quartz crystal is 13.7 mm; the gold electrode diameter is 5 mm. The morphological characterization of PNF, MWCNTs and MWCNTs–PNF films was done by means of scanning electron microscopy (SEM) (Hitachi S-3000H) and atomic force microscopy (AFM) (Being Nano-Instruments CSPM4000). All the measurements were carried out at 25 °C (±2).

2.3. Dispersion of MWCNTs and fabrication of MWCNTs–PNF composite film modified electrode

The important challenge in the preparation of MWCNTs was the difficulty in dispersing it in to homogeneous solution. Generally, the dispersion of CNTs has been carried out by physical (ultrasonication and milling) and chemical methods (covalent and non-covalent functionalization). These methods cause damage to CNTs and add impurities to them [37,38]. To overcome these drawbacks, dispersion of MWCNTs has been done by following the previous studies, which were conducted by Chun et al. [39]. Briefly, homogeneous dispersion of MWCNTs in ethanol solution was prepared using π-stacking interaction. The chemicals used for making the π-stacking complex were potassium as a doping material, phenanthrene as a non-polar molecule and 1,2-DME as a dipole solvent. About 50 mg of MWCNT was added to the solvent complex of 1,2-DME solution (20 mL) containing 0.2 mol dm^{-3} phenanthrene. The reaction mixture was stirred using a magnetic bar at 400 rpm at room temperature (25 ± 2 °C) for 48 h. The resulting doped MWCNTs were washed thoroughly with ethanol and water for several times and dried. Then the obtained MWCNTs (10 mg) in 10 mL ethanol were sonicated for 30 min to get uniform dispersion.

Before starting each experiment, GCEs were polished by BAS polishing kit with 0.05 μm alumina slurry, rinsed and then ultrasonicated in double distilled deionized water. The GCEs studied were uniformly coated with 50 μg cm^{-2} of MWCNTs and dried at about 40 °C. The electropolymerization of NF was done by electrochemical oxidation of NF (0.1 mM) on MWCNTs modified GCEs using pH 4 aqueous solution. It was performed by consecutive CV over a suitable potential range of 0.1–0.9 V. The optimization of PNF growth potential has been determined by various studies with different electropolymerization potentials (figures not shown). The obtained MWCNTs–PNF modified GCEs were washed carefully in deionized water to remove NF present on the modified GCE, and then dried at room temperature.

3. Results and discussions

3.1. Preparation and electrochemical characterizations of MWCNTs–PNF composite film

The electropolymerization of NF (0.1 mM) using consecutive CVs on MWCNTs modified GCE in KHP aqueous solution has been preformed for the preparation of MWCNTs–PNF composite film. Fig. 1(A) represents the electropolymerization of NF on MWCNTs modified GCE. The redox peak potential of PNF is at $E^{0\prime} = 0.25$ V versus Ag/AgCl. On subsequent cycles, the redox peak has been found growing. This result indicates that during the cycle, deposition of PNF takes place on MWCNTs modified GCE surface. Before transferring the film in to KHP for other electrochemical characterizations, the prepared composite film has been washed carefully in deionized water for removing NF present on the film. Initially, there were two different film modified GCEs studied as given in Fig. 1(B). The two different types are (a) MWCNTs–PNF and (b) PNF. The corresponding CVs have been measured at 20 mV s^{-1} scan rate in the potential range of 0.55–0.1 V. The redox peak current at $E^{0\prime} = 0.25$ V represents the redox reaction of PNF. From Fig. 1(B), it is found that the presence of MWCNTs shows catalytic effect on PNF redox peak currents. Further, the presence of MWCNTs in the composite film increases the overall back ground current. These results are evident with the active surface coverage concentration (Γ) given in Table 1 where, Γ of PNF is enhanced at MWCNTs film modified GCE when comparing at bare GCE. The calculated values from the same table shows that, MWCNTs enhances Γ of PNF by 0.8 pmol cm^{-2} μg^{-1}; and the overall increase in percentage of PNF Γ at MWCNTs film is 176.5%. In these Γ calculations, the number of electrons involved in PNF redox reaction is assumed as two. Similarly, the comparison of MWCNTs–PNF and only PNF on gold and ITO electrodes are given in Fig. 2(A and B) respectively, which show that MWCNTs catalyze the PNF electropolymerization.

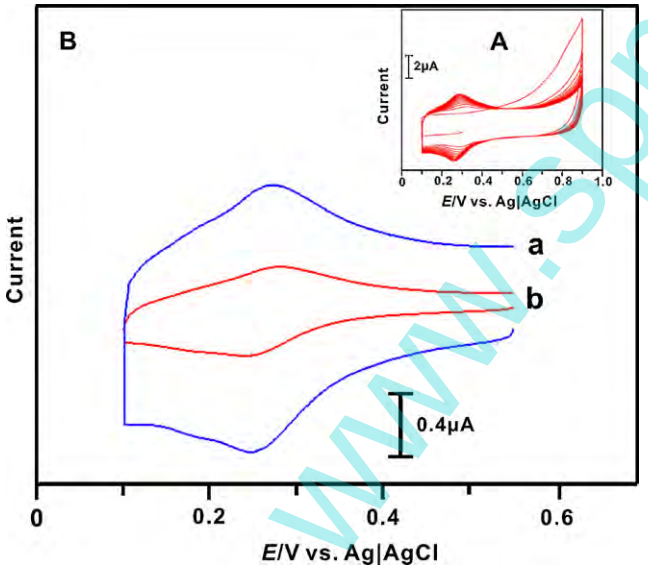

Fig. 1. (A) Repetitive CVs of MWCNTs-GCE modified from 0.1 mM NF in pH 4 KHP buffer, scan rate at 50 mV s^{-1}. (B) Comparison of CVs of (a) MWCNTs–PNF and (b) PNF films at GCE in pH 4.0 KHP buffer, scan rate at 20 mV s^{-1}.

Table 1
Surface coverage concentration (Γ) of PNF at different types of modified and unmodified electrodes using CV technique in pH 4.

Types of film modified electrodes	Γ (pmol cm^{-2})
PNF on bare GCE	21.7
PNF with MWCNTs-GCE	60.0
PNF on bare Au	27.8
PNF with MWCNTs-Au	99.3
PNF on bare ITO	10.3
PNF with MWCNTs-ITO	58.3

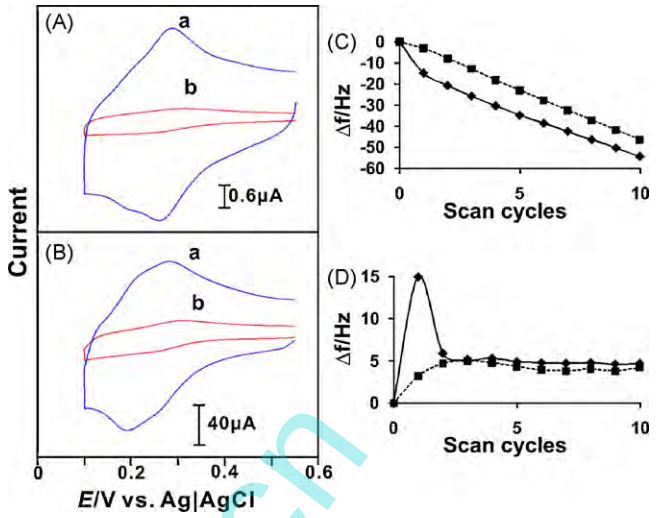

Fig. 2. Comparison of CVs of (a) MWCNTs–PNF and (b) PNF films at (A) gold and (B) ITO electrodes in pH 4 KHP buffer respectively, scan rate at 20 mV s^{-1}. (C) Plot of frequency change in EQCM vs. scan cycles and (D) every cycle frequency change vs. scan cycles for both the films, where dotted lines represents PNF and continuous lines represents MWCNTs–PNF film.

The EQCM experiments have been carried out by modifying the gold in electrochemical quartz crystal with uniformly coated MWCNTs and then dried at 40 °C. The increase in voltammetric peak current of PNF redox couple and the frequency decrease (or mass increase) are found to be consistent with the growth of PNF film on MWCNTs modified gold electrode (figures not shown). These results too show that the obvious deposition potential has started between 0.9 and 0.1 V. From the frequency change, the change in the mass of composite film at the quartz crystal can be calculated by the Sauerbrey Eq. (1), however 1 Hz frequency change is equivalent to 1.4 ng cm^{-2} of mass change [40,41]. The mass change during PNF incorporation on MWCNTs modified and unmodified gold electrodes for total cycles are 76.5 and 65.1 ng cm^{-2} respectively.

$$\text{Mass change}\,(\Delta m) = -\tfrac{1}{2}(f_0^{-2})(\Delta f)A(K\rho)^{1/2} \quad (1)$$

where f_0 is the oscillation frequency of the crystal; Δf is the frequency change; A, the area of gold disk; K the shear modulus of the crystal; ρ the density of the crystal. Fig. 2(C) indicates the variation of frequency with increase of scan cycles for PNF at MWCNTs modified (continuous line) and unmodified (dotted line) EQCM gold crystal electrodes. Fig. 2(D) indicates every cycle of frequency with the increase of scan cycles for PNF at MWCNTs modified (continuous line) and unmodified (dotted line) EQCM gold crystal electrodes. These EQCM results prove that the deposition of PNF on the MWCNTs film is more stabilized and more homogeneous than on the bare gold electrode.

3.2. Topographic characterization of MWCNTs–PNF using SEM and AFM

Three different films: only PNF, MWCNTs and MWCNTs–PNF have been prepared on indium tin oxide (ITO) with similar conditions and similar potential as that of GCE and have been characterized using SEM and AFM. From Fig. 3, it is significant that there are morphological differences between only PNF, MWCNTs and PNF coated MWCNTs films. All the three images have

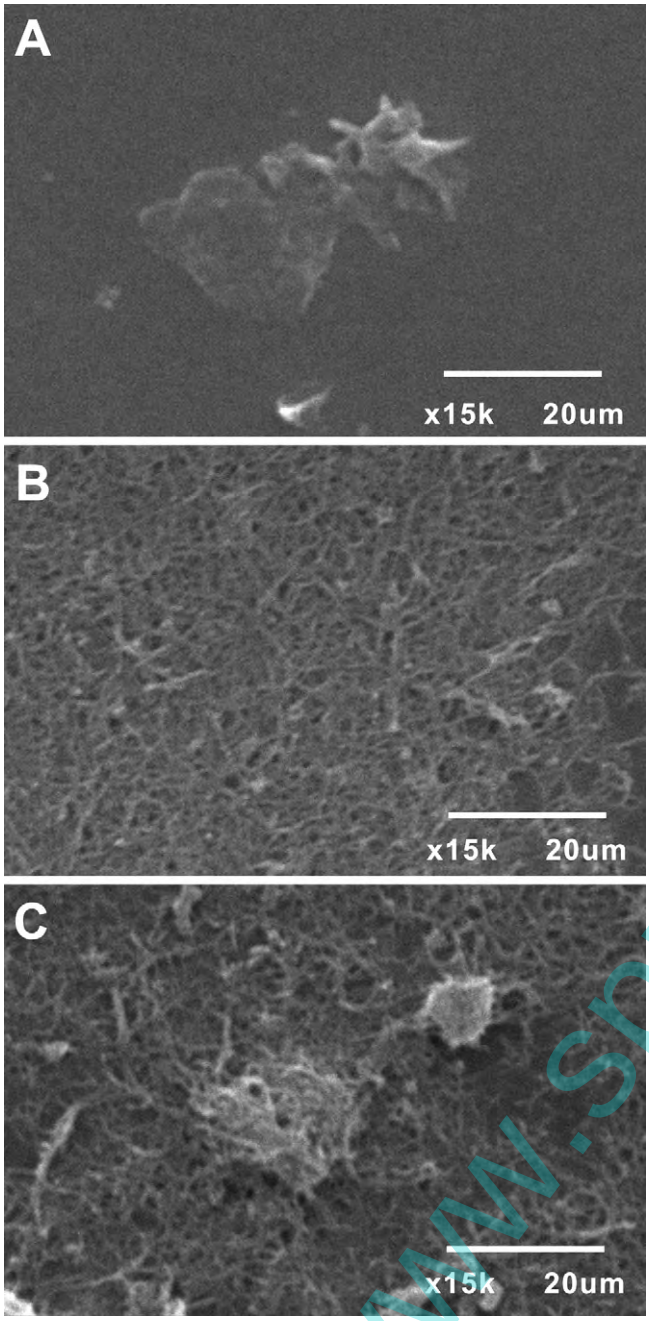

Fig. 3. SEM images of (A) PNF, (B) MWCNTs and (C) MWCNTs–PNF films.

been measured at the same resolution of about ×15k. The top views of structures Fig. 3(A and B) on the ITO electrode surface shows PNF deposition, and uniformly coated undamaged MWCNTs respectively. The deposition of PNF on ITO has taken place with patches in different sizes (not shown in figure), which is not as much uniform as MWCNTs on ITO. In Fig. 3(A), only a well formed PNF patch is shown. Fig. 3(C) indicates the deposition of PNF, which covered over MWCNTs. This Fig. 3(C) shows an obvious formation of MWCNTs–PNF composite film on ITO. Where, the PNF deposition over MWCNTs is more uniform than the PNF on ITO. Similarly, Fig. 4(A–C) shows the AFM images of only PNF, MWCNTs and MWCNTs–PNF respectively. The AFM images reveal that the MWCNTs and MWCNTs–PNF films have higher thickness than the PNF film. These AFM results are similar to SEM results.

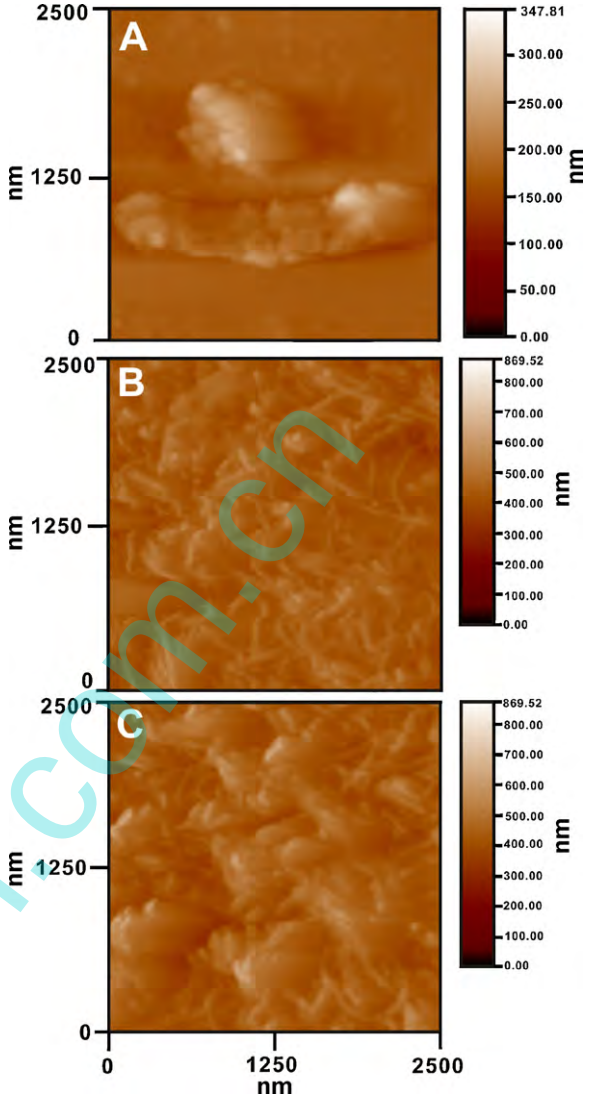

Fig. 4. AFM images of (A) PNF, (B) MWCNTs and (C) MWCNTs–PNF films.

3.3. Electrochemical studies of MWCNTs–PNF composite film

The CVs of MWCNTs–PNF composite film on GCE in pH 4 at different scan rates show that the anodic and cathodic peak currents of the composite film's redox couple, which increases linearly with the increase of scan rates (figure not shown). The ratio of Ipa/Ipc from the Fig. 5(A) demonstrates that the redox process is not controlled by diffusion. However, the ΔEp of each scan rate reveals that the peak separation of composite's redox couple increases as the scan rate increase (figure not shown). From the slope values of ΔE vs. log scan rate, by assuming the value of $\alpha \approx 0.5$, number of electrons involved as two, the electron transfer rate constant (k_s) has been calculated using the Eq. (2) based on Laviron theory [42]. The k_s values are 0.49 and 2.18 s^{-1} for PNF and MWCNTs–PNF modified GCEs respectively. From these k_s values, we have calculated the increase in the ability of electron transfer between the electrode surface and PNF in presence of MWCNTs, and it is ≈346%. These results show the enhanced functional property of composite film in the presence of MWCNTs.

$$\log k_s = \alpha \log(1-\alpha) + (1-\alpha)\log\alpha - \log\left(\frac{RT}{nF\upsilon}\right) - \alpha(1-\alpha)\frac{nF\Delta E}{2.3RT} \quad (2)$$

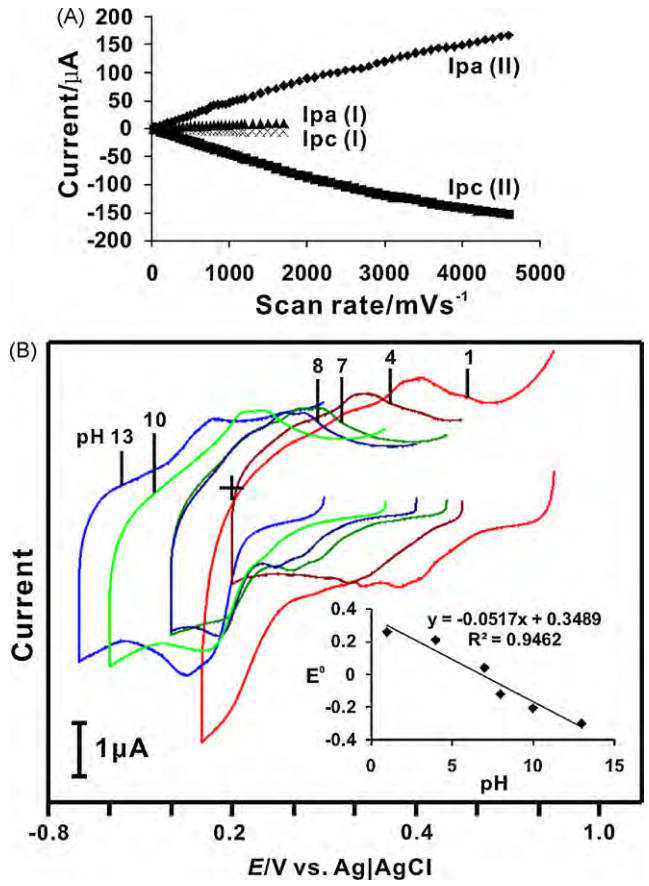

Fig. 5. (A) Shows the plot of Epa and Epc vs. different scan rate for both (I) PNF and (II) MWCNTs–PNF composite film present in pH 4 KHP buffer. (B) CVs of the MWCNTs–PNF composite film synthesized from 0.1 mM NF in pH 4 KHP buffer and then, it was transferred to various pH solutions; scan rate: 20 mV s^{-1}. The inset in (B) shows the formal potential vs. pH (1–13), the slope −51 mV pH^{-1} is almost nearer to Nernstian equation for equal number of electrons and protons transfer.

In the Eq. (2), the scan rate and ΔE values are in unit volts. Fig. 5(B) shows the CVs of MWCNTs–PNF on GCE obtained in pH 4 aqueous solution, then washed with deionized water, and was transferred to various pH aqueous buffer solutions without the presence of NF. The results show that the film is highly stable in the pH range between 1 and 13. The values of Epa and Epc depend on the pH value of buffer solution. The inset in Fig. 5(B) shows the formal potential of MWCNTs–PNF plotted over the pH range from 1 to 13. The response shows a slope of −51 mV pH^{-1}, which is close to that given by Nernstian equation for equal number of electrons and protons transfer. All these above results show the enhanced functional properties of the composite film in the presence of both PNF and MWCNTs.

3.4. Electrocatalysis and voltammetric resolution of analytes present individually and in the mixture at PNF, MWCNTs and MWCNTs–PNF film modified electrodes using CV technique

The electrochemical oxidation of AD, GU and THY at MWCNTs–PNF composite films have been carried out using pH 7.4 PBS at 20 mV s^{-1} in the potential range of −0.3 to 1.4 V as given in Fig. 6(A–C). All the CVs have been recorded at the constant time interval of 2 min with nitrogen purging before the start of each experiment. The CVs for MWCNTs–PNF film exhibits a redox couple in the absence of analytes, upon addition of AD, GU and THY (individually on separate film modified GCEs) a new growth in

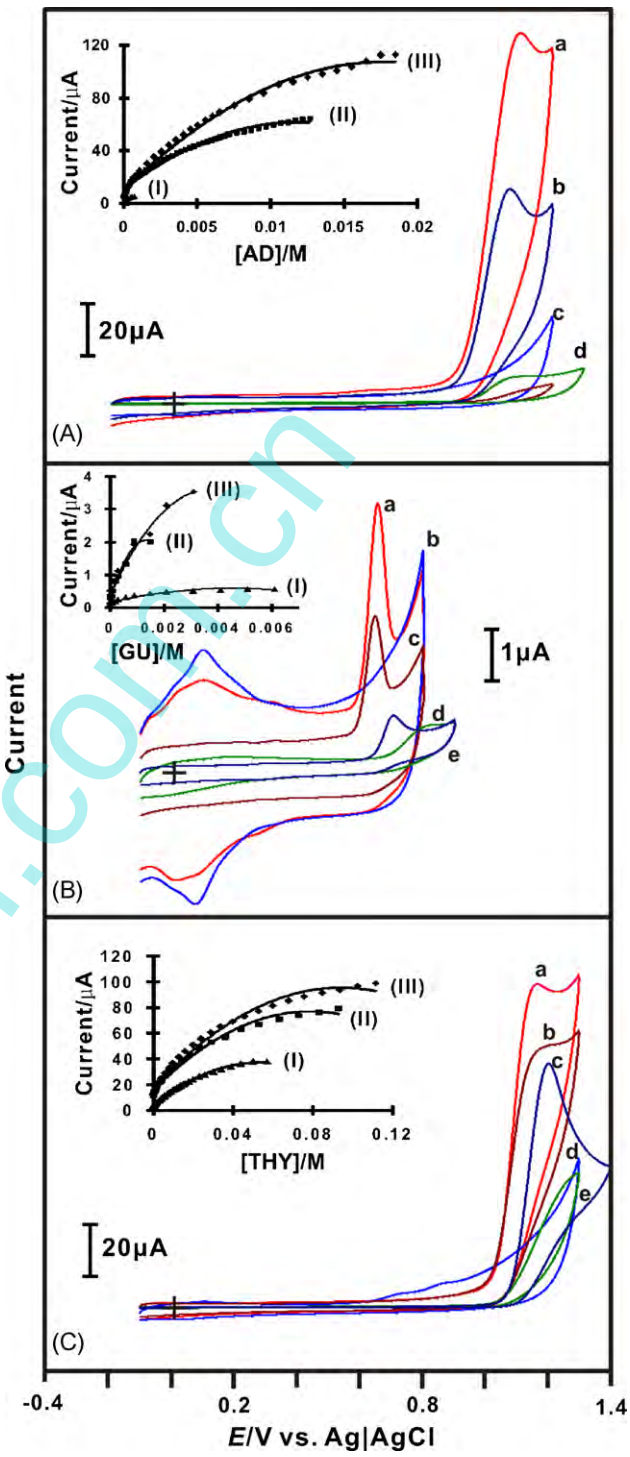

Fig. 6. CVs of (A) AD, (B) GU and (C) THY at various electrodes using pH 7.4 PBS at 20 mV s^{-1}; (a and d) the highest and lowest concentration of the analytes at MWCNTs–PNF, (b, e and c) the highest concentration of analyte mixture at MWCNTs, PNF film modified GCE and bare GCE respectively. The highest and lowest concentrations of analytes are given in Table 2. The insets in all figures are the plots of peak current vs. concentration, where (I), (II) and (III) are PNF, MWCNTs and MWCNTs–PNF films.

the oxidation peak of respective analytes appears at the Epa values given in Table 2. From these Epa values, it is obvious that the GU appears at lower positive potential than AD, which is at lower potential than THY. An increase in concentration of AD, GU and THY, simultaneously produces a linear increase in the oxidation peak currents of all the three analytes with good film stability as shown in

Table 2
Electroanalytical results for AD, GU and THY individually at MWCNTs–PNF composite film using CV technique.

Analytes	Epa (mV)	Ipa (μA)	Concentration range (mM)		Detection limit (μM)[a]	Sensitivity (mA M^{-1} cm^{-2})[b]
			Low	High		
GU	651.8	3.52	0.02	3.1	18.2	13.4 [0.9537]
AD	1040.4	112.5	0.01	18.6	8.6	74.33 [0.9341]
THY	1167.9	98.84	0.02	112.1	19.4	10.57 [0.9039]

[a] At a signal to noise ratio of 3.
[b] The correlation coefficients are given in parentheses.

the inset plots from Fig. 6(A–C). The detection limits for each analyte using CV at a signal to noise ratio of 3 are given in Table 2. The detection limit and concentration range for each analyte almost covers the concentration range found in the physiological conditions. From the slopes of the linear calibration curves in Fig. 6 the sensitivity and their correlation coefficients of MWCNTs–PNF modified GCE towards the analytes have been calculated and are given in Table 2. Similarly, the Ipa values from the same table shows that the peak current of GU is lower when compared to other two analytes. Both these results lower in sensitivity and peak current of GU are depends upon its diffusion property at the composite film, where GU has lower solubility and diffusion than the other analytes. Indeed, the diffusion of analytes is one of the important influencing factors in electrocatalysis. The previous studies have reported also that GU is absorbed on the surface of electrode causing the electrode process dependent on adsorption [43].

Fig. 7(A) depicts the electrochemical oxidation CVs that have been obtained for AD, GU and THY coexisting (analyte mixture) at MWCNTs–PNF film using pH 7.4 PBS at 20 mV s^{-1} in the potential range of −0.3 to 1.4 V; where (a) and (c) represent highest and lowest concentration of the analyte mixture at MWCNTs–PNF composite film. (b), (e) and (d) represent the highest concentration of the analyte mixture at MWCNTs, PNF film modified GCE and bare GCE respectively. The CVs of bare GCE in Fig. 7(A) exhibits only one broad peak, here the broad peak represents the voltammetric signal of the analyte mixture. Moreover, the peak current decreases in the subsequent cycles for both PNF film and bare GCE. These observations clearly indicate both PNF film and bare GCE fail to separate the voltammetric signals of analytes in mixture. The fouling effect of the electrode surface with the oxidized products of analytes is the reason for obtaining the weak single peak for analytes in the mixture [44]. The CVs for MWCNTs–PNF exhibits a redox couples in the absence of the analytes, upon the addition of analyte mixture, as shown in Fig. 7(A) a new growth in the oxidation peaks of respective analytes appears at Epa given in Table 3. An increase in concentration of analyte mixture simultaneously produces a linear increase in the oxidation peak currents of all the three analytes with good film stability as shown in Fig. 7(A). The peak separation values between analytes are given in Table 4. The Ipa values from Table 3 obviously shows that the anodic peak current of each analyte at MWCNTs–PNF is higher than that of MWCNTs, which reveals that PNF's redox reaction involves and enhances the peak current of analytes. In these results, the increase in current and decrease in potential, both are considered as the electrocatalysis [6]. The comparison of linear increase of analyte concentration vs. peak current between MWCNTs and MWCNTs–PNF are shown in Fig. 7(B, C and D). The detection limits of analytes at MWCNTs and MWCNTs–PNF using CV at a signal to noise ratio of 3 are given in Table 3. These results show that the detection of analytes at MWCNTs–PNF is possible at lower concentration when comparing to that at MWCNTs alone. From the slopes of the linear calibration curves, sensitivity of the MWCNTs and MWCNTs–PNF modified GCEs and their correlation coefficients have been calculated and where given in Table 3. In these results too, the sensitivity of MWCNTs–PNF is higher than MWCNTs for all the three analytes. From all these above results it

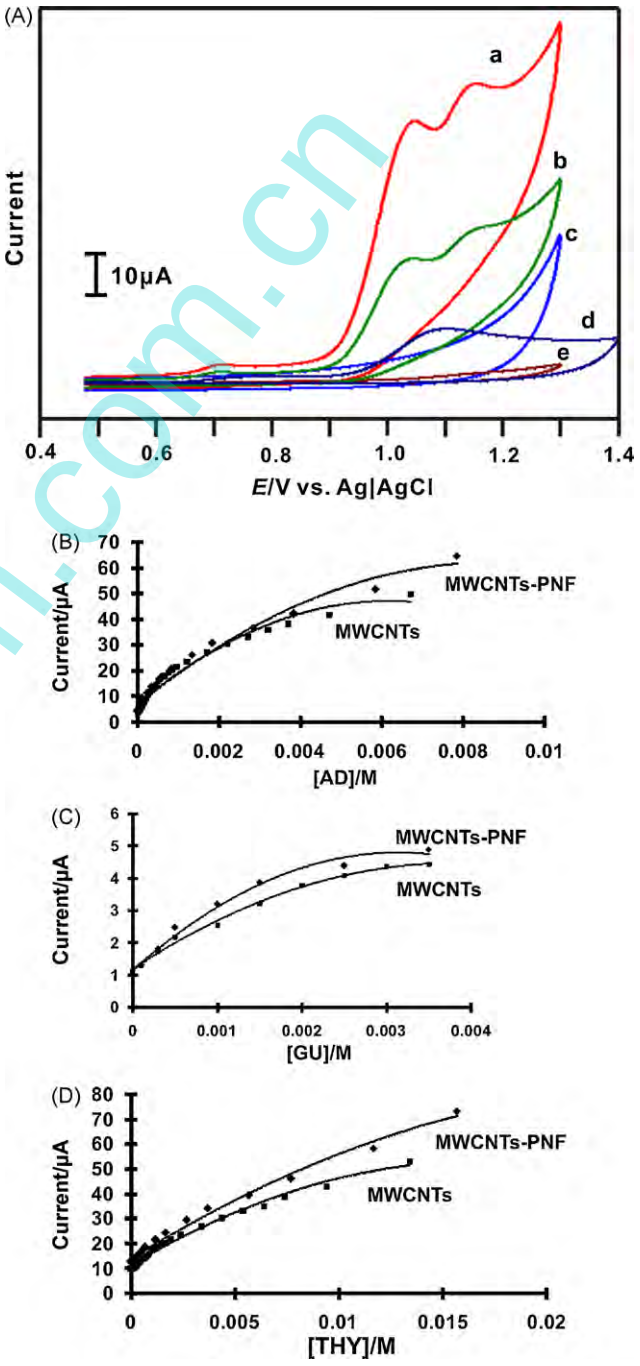

Fig. 7. (A) CVs of AD, GU and THY present in analyte mixture at various electrodes using pH 7.4 PBS at 20 mV s^{-1}; (a and c) the highest and lowest concentration of the analytes at MWCNTs–PNF, (b, e and d) the highest concentration of the analyte mixture at MWCNTs, PNF film and bare GCE respectively. The highest and lowest concentrations of analytes are given in Table 3. (B, C and D) The plots of peak current vs. concentrations of AD, GU and THY respectively, at MWCNTs and MWCNTs–PNF films.

Table 3
Electroanalytical results for AD, GU and THY present in the mixture of analytes at different film modified electrodes using CV technique.

Analytes	Epa (mV)	Ipa (μA)	Concentration range (mM)		Detection limit (μM)[a]	Sensitivity (mA M^{-1} cm^{-2})[b]
			Low	High		
GU[c]	714.2	4.417	0.1	3.5	98.56	12.22 [0.9517]
GU[d]	707.3	4.869	0.1	3.5	96.84	13.58 [0.8922]
AD[c]	1057.3	49.47	0.01	6.7	9.2	89.31 [0.8933]
AD[d]	1027.6	64.42	0.01	7.9	7.9	95.90 [0.9404]
THY[c]	1160.3	53.02	0.02	13.4	19.3	41.92 [0.9596]
THY[d]	1153.4	73.17	0.02	15.7	16.8	48.14 [0.9797]

[a] At a signal to noise ratio of 3.
[b] The correlation coefficients are given in parentheses.
[c] MWCNTs film modified GCE.
[d] MWCNTs–PNF composite film modified GCE.

is clear that MWCNTs–PNF composite film is more efficient when comparing with MWCNTs alone.

3.5. Voltammetric resolution of the analytes present in the mixture at MWCNTs and MWCNTs–PNF film modified electrodes using DPV technique

The DPVs have been obtained during simultaneous change of the concentrations of analyte mixture at MWCNTs–PNF modified GCE using 0.1 M pH 7.4 PBS, as shown in Fig. 8; where (A) is at MWCNTs–PNF and (B) MWCNTs modified GCEs. The DPVs have been recorded at a constant time interval of 2 min with nitrogen purging before the start of each experiment. Interestingly, the peak currents for AD and THY increases linearly with the increase of analyte mixture's concentration, while for GU; the peak current is not higher when comparing AD and THY. This phenomenon occurs due to the diffusion of GU through the composite film is much slower when compared with that of other two analytes [45]. They demonstrate the calibration curves (figures not shown) for analyte mixture, which are almost linear for a wide range of concentrations as shown in Table 5. The detection limit of MWCNTs–PNF film modified electrodes using DPVs are given in the same table at a signal to noise ratio of 3, which covers the concentration range found in the physiological conditions. From the slopes of the linear calibration curves, the sensitivity of MWCNTs–PNF modified GCE and their correlation coefficients have been calculated as given in Table 5. All these values show higher efficiency of the MWCNTs–PNF towards the analytes when comparing only MWCNTs.

3.6. Electroanalysis of ssDNA at MWCNTs–PNF film modified electrode using SDCV and DPV

The electrochemical oxidation of AD, GU and THY present in ssDNA at MWCNTs–PNF composite film have been carried out using pH 13 KOH as shown in Fig. 9. Fig. 9(A) depicts the electrochemical oxidation SDCVs that have been obtained for ssDNA at 20 mV s^{-1} in the potential range of −0.3 to 1.4 V, where the CVs obtained during simultaneous change of the ssDNA concentration were converted in to semi-derivative (SD) current. Interestingly, the peak current represents AD (Epa = 900 mV) and THY (Epa = 1040 mV) increases with the increase of ssDNA concentration in the range of 12–102 μM. However, there is no peak separation until 72 μM and there is no peak detected for GU. From the slopes of linear calibration curves (Fig. 9(A), inset), the sensitivity of MWCNTs–PNF for AD and THY have been calculated, and they are 4.6 and 4.5 mA mM^{-1} cm^{-2}

Table 4
Peak separation between AD, GU and THY present in the mixture of analytes at different film modified electrodes using different techniques.

Types of film modified electrodes[a]	pH	Peak separation (mV)	
		GU–AD	AD–THY
CV[b]	7.4	343.1	103
CV[c]		320.3	132.7
DPV[b]	7.4	318.9	112.4
DPV[c]		312.5	120.2

[a] The films have been modified on GCE.
[b] MWCNTs film modified GCE.
[c] MWCNTs–PNF composite film modified GCE.

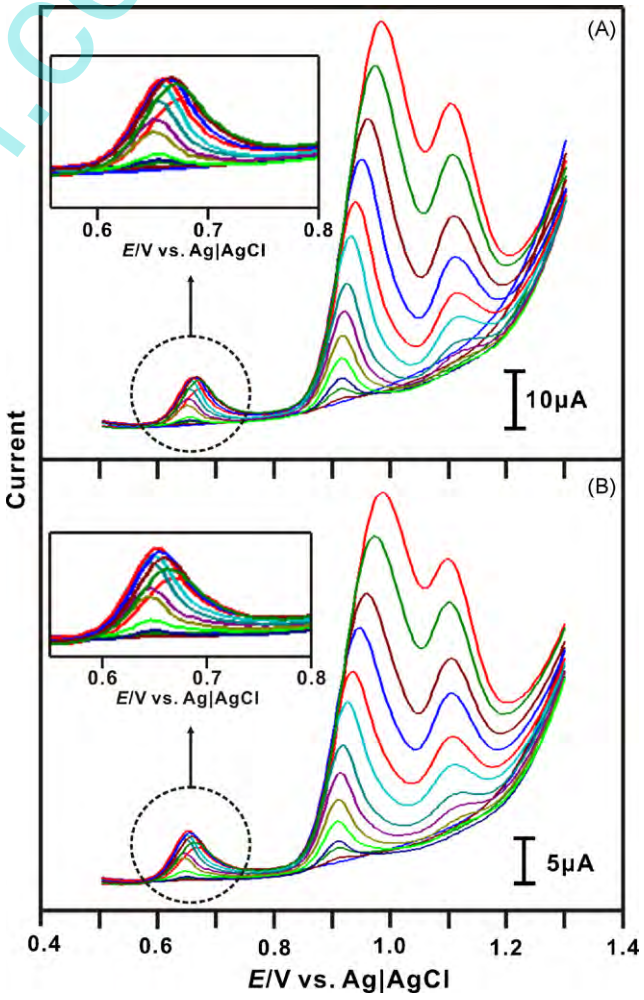

Fig. 8. DPVs of AD, GU and THY present in analyte mixture at (A) MWCNTs–PNF and (B) MWCNTs using pH 7.4 PBS. The concentration ranges of each analytes are given in Table 5.

Table 5
Electroanalytical results for AD, GU and THY present in the mixture of analytes at MWCNTs–PNF film modified GCEs using DPV technique.

Analytes	Epa (mV)	Ipa (μA)	Concentration range (mM)		Detection limit (μM)[a]	Sensitivity (mA M^{-1} cm^{-2})[b]
			Low	High		
GU[c]	667.6	5.416	0.1	8.5	97.92	8.5 [0.8552]
GU[d]	670.2	7.967	0.1	8.5	95.76	12.62 [0.8738]
AD[c]	986.5	42.2	0.01	3.9	8.7	133.33 [0.8941]
AD[d]	982.7	70.12	0.01	3.9	7.4	218.18 [0.8946]
THY[c]	1098.9	35.21	0.02	7.7	18.7	51.2 [0.9754]
THY[d]	1102.9	55.53	0.02	7.7	16.2	78.22 [0.9907]

[a] At a signal to noise ratio of 3.
[b] The correlation coefficients are given in parentheses.
[c] MWCNTs film modified GCE.
[d] MWCNTs–PNF composite film modified GCE.

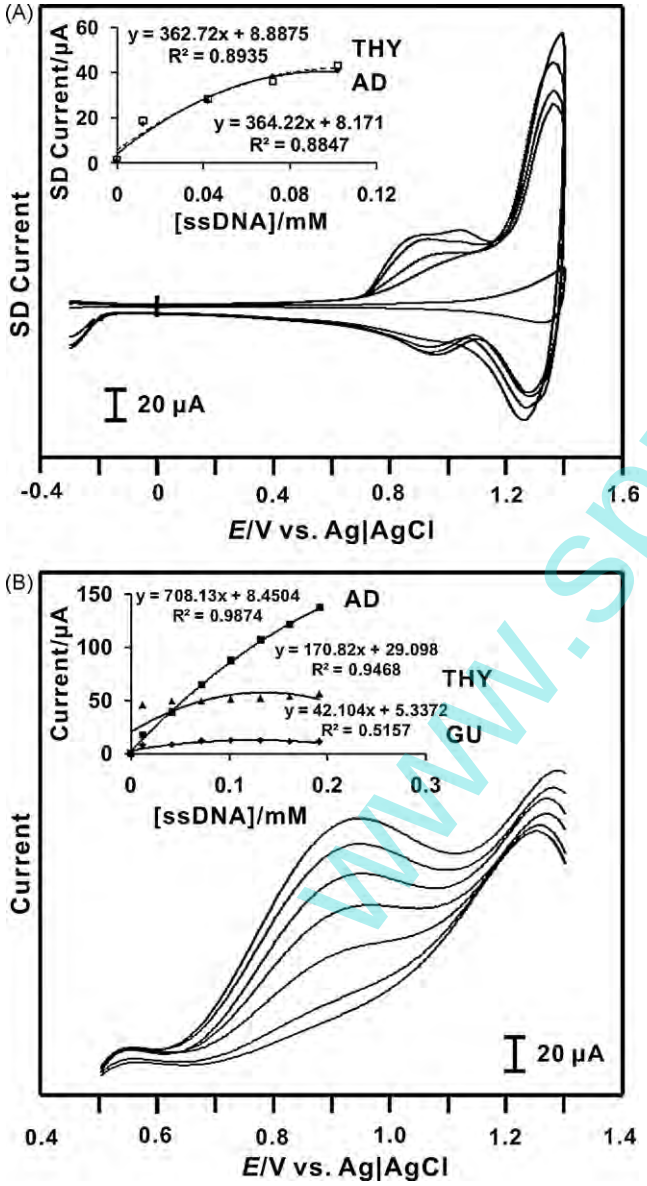

Fig. 9. (A) SDCVs of MWCNTs–PNF film in pH 13 KOH aqueous solution with various concentration of ssDNA = 0 and 12 to 102 μM; where scan rate = 20 mV s^{-1}. The inset in (A) shows the plot of SD current vs. different concentration of ssDNA. (B) DPVs of MWCNTs–PNF film in pH 13 KOH aqueous solution with various concentration of ssDNA = 12–192 μM. The inset in (B) shows the plot of current vs. different concentration of ssDNA.

respectively. Fig. 9(B) depicts the electrochemical oxidation DPVs that have been obtained for ssDNA in the potential range of 0.5–1.3 V. The DPVs shown in Fig. 9(B) have been recorded at a constant time interval of 2 min with nitrogen purging before the start of each experiment. The peak currents for AD (Epa = 950 mV) and THY (Epa = 1280 mV) increases linearly with the increase of ssDNA concentration, while for GU (Epa = 556 mV); the peak current is not higher when comparing AD and THY. This phenomenon is similar to the result discussed in the previous section. From the inset in Fig. 9(B), the sensitivity of MWCNTs–PNF film for AD, GU and THY have been calculated and they are 0.71, 0.04 and 0.17 mA mM^{-1} cm^{-2} respectively. These above SDCV and DPV results shows that MWCNTs–PNF can be used for the simultaneous determination of AD, GU and THY present in ssDNA.

4. Conclusions

We have developed a novel composite material made of MWCNTs and PNF (MWCNTs–PNF) at GCE, Au and ITO electrodes, which are stable in aqueous solutions. The developed composite film for the simultaneous determination combines the advantages of ease of fabrication, high reproducibility and sufficient long-term stability. The EQCM results confirmed the incorporation of PNF on MWCNTs, and the SEM and AFM results show the difference between combinations of MWCNTs and PNF film's morphology. Further, MWCNTs–PNF composite film has excellent functional properties with good catalytic activity on AD, GU and THY. The experimental method of CV, SDCV and DPV with composite film biosensor integrated into a GCE presented in this paper provides an opportunity for qualitative, quantitative characterization and simultaneous determination of AD, GU and THY present in ssDNA. At the same time, the oxidized electrodes alleviate fouling problems; good repeatability of the voltammograms and stability. Therefore, this work establishes and illustrates, in principle and potential, a simple and novel approach for the development of a simultaneous AD, GU and THY voltammetric sensor based on modified GCE.

Acknowledgement

This work was supported by the National Science Council and the Ministry of Education of Taiwan (Republic of China).

References

[1] C.P. McMahon, G. Rocchitta, S.M. Kirwan, S.J. Killoran, P.A. Serra, J.P. Lowry, R.D. O'Neill, Biosens. Bioelectron. 22 (2007) 1466.
[2] I. Becerik, F. Kadirgan, Synth. Met. 124 (2001) 379.
[3] T. Selvaraju, R.R. Ramaraj, J. Electroanal. Chem. 585 (2005) 290.

[4] M. Mao, D. Zhang, T. Sotomura, K. Nakatsu, N. Koshiba, T. Ohsaka, Electrochim. Acta 48 (2003) 1015.
[5] M. Yasuzawa, A. Kunugi, Electrochem. Commun. 1 (1999) 459.
[6] C.P. Andrieux, O. Haas, J.M. SavGant, J. Am. Chem. Soc. 108 (1986) 8175.
[7] A.A. Karyakin, E.E. Karyakina, H.L. Schmidt, Electroanalysis 11 (1999) 149.
[8] A.G. MacDiarmid, J.C. Chiang, A.G. Richter, A. Epstein, Synth. Met. 18 (1987) 285.
[9] Y. Li, R. Qian, Synth. Met. 28 (1989) 127.
[10] K. Tanaka, S. Ikeda, N. Oyama, K. Tokuda, T. Ohsaka, Anal. Sci. 9 (1993) 783.
[11] J. Ghasemi, D.E. Mohammadi, J. Microchem. 71 (2002) 1.
[12] J.M. Bastidas, P. Pinilla, E. Cano, J.L. Polo, S. Miguel, Corros. Sci. 45 (2003) 427.
[13] W. Bae, R.K. Mehra, J. Inorg. Biochem. 70 (1998) 125.
[14] S.M. Chen, Y.H. Fa, J. Electroanal. Chem. 553 (2003) 63.
[15] S.M. Chen, Y.H. Fa, J. Electroanal. Chem. 567 (2004) 9.
[16] S.M. Chen, Y.H. Fa, Electroanalysis 17 (2005) 579.
[17] H. Ashassi-Sorkhabi, D. Seifzadeh, J. Appl. Electrochem. 38 (2008) 1545.
[18] T. Yang, Z.J. Wang, K. Jiao, Q.J. Li, Chem. Res. Chin. Univ. 22 (2006) 292.
[19] J. Wang, M. Musameh, Anal. Chim. Acta 511 (2004) 33.
[20] H. Cai, X. Cao, Y. Jiang, P. He, Y. Fang, Anal. Bioanal. Chem. 375 (2003) 287.
[21] A. Erdem, P. Papakonstantinou, H. Murphy, Anal. Chem. 78 (2006) 6656.
[22] Q. Li, J. Zhang, H. Yan, M. He, Z. Liu, Carbon 42 (2004) 287.
[23] J. Zhang, J.K. Lee, Y. Wu, R.W. Murray, Nano Lett. 3 (2003) 403.
[24] M. Zhang, K. Gong, H. Zhang, L. Mao, Biosens. Bioelectron. 20 (2005) 1270.
[25] R.J. Chen, Y. Zhang, D. Wang, H. Dai, J. Am. Chem. Soc. 123 (2001) 3838.
[26] J. Wang, J. Dai, T. Yarlagadda, Langmuir 21 (2005) 9.
[27] M. Tahhan, V.T. Truong, G.M. Spinks, G. GWallace, Smart Mater. Struct. 12 (2003) 626.
[28] Q. Xu, S.F. Wang, Microchim. Acta 151 (2005) 47.
[29] E.E. Ferapontova, Electrochim. Acta 49 (2004) 1751.
[30] N.R.D. Tacconi, K. Rajeshwar, R.O. Lezna, Chem. Mater. 15 (2003) 3046.
[31] B.D. Humphrey, S. Sinha, A.B. Bocarsly, J. Phys. Chem. 91 (1987) 586.
[32] G. Dryhurst, Talanta 19 (1972) 769.
[33] S.H. Lim, J. Wei, J. Lin, Chem. Phys. Lett. 400 (2004) 578.
[34] U. Yogeswaran, S. Thiagarajan, S.M. Chen, Carbon 45 (2007) 2783.
[35] K. Kerman, Y. Morita, Y. Takamura, E. Tamiya, Electrochem. Commun. 5 (2003) 887.
[36] K.H. Choa, J. Choob, S.W. Jooc, J. Mol. Struct. 738 (2005) 9.
[37] J. Chen, M.A. Hamon, H. Hu, Y. Chen, A.M. Rao, P.C. Eklund, Science 282 (1998) 95.
[38] J. Chen, A.M. Rao, S. Lyuksyutov, M.E. Itkis, R.E. Smalley, R.C. Haddon, J. Phys. Chem. B 105 (2001) 2525.
[39] K.Y. Chun, S.K. Choi, H.J. Kang, C.Y. Park, C.J. Lee, Carbon 44 (2006) 1491.
[40] S.M. Chen, M.I. Liu, Electrochim. Acta 51 (2006) 4744.
[41] S.M. Chen, C.J. Liao, V.S. Vasantha, J. Electroanal. Chem. 589 (2006) 15.
[42] E. Laviron, J. Electroanal. Chem. 101 (1979) 19.
[43] Z. Wang, S. Xiao, Y. Chen, J. Electroanal. Chem. 589 (2006) 237.
[44] C.R. Raj, K. Tokuda, T. Ohsaka, Bioelectrochemistry 53 (2001) 183.
[45] V.S. Vasantha, S.M. Chen, J. Electroanal. Chem. 592 (2006) 77.